Contemporary Mathematics
http://ojs.wiserpub.com/index.php/CM/

Research Article

Modeling The Thermal Efficiency of Convex Parabolic Fins Using Ternary Nanofluids for Electronic Cooling Under LTNE Conditions

Manaswini R[1], S Manjunatha[1], Khalil Ur Rehman[2*], Tanuja T N[3], Wasfi Shatanawi[2]

[1] Department of Mathematics, CHRIST (Deemed to be University), Bengaluru-560076, Karnataka, India
[2] Department of Mathematics and Sciences, College of Sciences and Humanities, Prince Sultan University, Riyadh 11586, Saudi Arabia
[3] Department of Mathematics, Amity School of Applied Sciences, Amity University, Bengaluru-562110, Karnataka, India
E-mail: kurrehman@psu.edu.sa

Received: 15 September 2025; **Revised:** 9 December 2025; **Accepted:** 6 February 2026

Abstract: The present semi-analytical study examines the thermal behavior of a convex parabolic fin under totally wet conditions, taking both linear and non-linear internal heat generation into account. The Local Thermal Non-Equilibrium model (LTNE) which has a dual-equation framework describes the heat exchange between the solid and fluid phases. Hence, this technique is crucial for accurately capturing heat transfer in systems with notable temperature gradients in both the fluid and solid phases. To increase the thermal conductivity of the ethylene glycol-water mixture, nanoparticles Go, Ag and Cu are added. The governing energy equations are nondimensionalized by using dimensionless variables and solved using the Differential Transformation Method (DTM). The visual analysis is carried out to evaluate the system's thermal performance and efficiency by examining the key thermal parameters effect on the fin temperature profiles. The primary conclusions show that, in comparison to linear heat generation model, the combination of ternary nanofluids and nonlinear internal heat generation significantly increases the rate of heat transmission. Furthermore, wet porous effects and enhanced radiation alter the temperature and reduce fin efficiency by increasing resistance and heat loss. Hence, this work offers insights to enhance thermal management in wet cooling systems which are used in solar panels and electronic equipment.

Keywords: convex parabolic fin, Local Thermal Non-Equilibrium (LTNE) model, Linear and non-linear heat generation, ternary nanofluid, efficiency

MSC: 80A19, 80M20

Nomenclature

$a_{sf} = \frac{A_{sf}}{W\Delta x}$	Interfacial area per unit volume of porous fin (m^{-1})
g	Acceleration due to gravity (ms^{-2})
x	Axial coordinates (m)
X	Non-dimensional coordinate
h_{sf}	Convective heat transfer coefficient between solid and fluid phase
$A_c^* = wt$	Cross section area of the fin (m^{-2})

Copyright ©2026 Khalil Ur Rehman, et al.
DOI: https://doi.org/10.37256/cm.7420268644
This is an open-access article distributed under a CC BY license
(Creative Commons Attribution 4.0 International License)
https://creativecommons.org/licenses/by/4.0/

h_L	External convective heat transfer coefficient ($Wm^{-2}K^{-1}$)
p	Perimeter of cross section (m)
q	Heat generation (Wm^{-3})
L	Length (m)
w	Width (m)
Q	Heat generation number
C_p	Specific heat capacitance ($Jkg^{-1}K^{-1}$)
$Bi = \frac{a_{sf}h_{sf}L^2}{(1-\varphi)k_s} = \frac{a_{sf}h_{sf}L^2}{\varphi k_s}$	Biot number
$Nr = \frac{4\sigma\varepsilon^* F_{f-a}T_\infty^3 L}{(1-\varphi)k_f}$	Surface-ambient radiation parameter
$R = \frac{4\sigma T_\infty^3}{3\beta_R(1-\varphi)k_s}$	Radiation conduction parameter
$Nc = \frac{\left(\rho C_p\right)_f gK(\rho\beta)_f w(T_b - T_\infty)}{\phi\mu_f k_f}$	Rayleigh number
tnf	Ternary nanofluid
i_{fg}	Latent heat of evaporation (Jkg^{-1})
b	Base of fin
M^*	Mass transfer (kgs^{-1})
LTNE	Local Thermal Non-Equilibrium model

Greek symbols

β_R	Rosseland means extinction coefficient (m)
$\theta_f, \theta_s, \Theta_f, \Theta_s$	Dimensionless temperature
μ	Dynamic viscosity ($kgm^{-1}s^{-1}$)
η	Fin efficiency
ρ	Density (kgm^{-3})
$\chi = \frac{h_L L}{k_f}$	External convective parameter
σ	Stefan-Boltzmann constant (Wm)
v_w	Velocity (ms^{-1})
φ	Porosity
τ	Thickness (m)
ε^*	Emissivity coefficient

1. Introduction

Fins are essential components of complex heat management systems as they boost thermal efficiency through expanding the surface area available for heat transmission. These fins are widely used to increase the rate of heat dissipation in systems such as heat exchangers, pipelines for the transfer of oil and chemical processing equipment. For instance, a laptop's processor has thin metal fins that helps to disperse heat. Here, air is blown over these fins by a fan, which quickly removes heat and keeps the processor cool. Thus, fins enhance heat dissipation, ensuring equipment works safely and effectively. Harper and Brown [1] were the first to mathematically capture how heat flows through an extended surface, not only by conduction along the material but also by convection into the surrounding fluid. Norris and Spofford [2] analyzed the forced-convection heat transfer in tiny discontinuous fin arrays. Furthermore, adding porosity to the fin design improves thermal performance by increasing surface area and encouraging improved airflow, which makes heat transmission more effective. Porous fins are superior to solid fins for improved heat transfer and material efficiency, as demonstrated by Kiwan and Al-Nimr [3]. Saedodin and Sadeghi [4] employ energy balance and Darcy's model to investigate long porous and solid fins in natural convection. Hatami and Ganji [5] studied the both heat and mass transfer

aspects in circular porous fins. Gorla and Bakier [6] studied the heat transfer in a porous rectangular fin while accounting for radiation and convection.

The impact of various fin shapes on heat transfer performance has been the subject of numerous studies due to the growing interest in fin technology. Madhavadas et al. [7] critically analyzed a variety of fin profiles, including circular pin, wavy, plain rectangle, and rectangular pin fins. Study found that the heat transmission efficiency is greatly influenced by fin type, shape and thermo-geometry. Ravikumar and Raj [8] deliberated that; how two different fin profiles affect a tube heat exchanger's ability to transmit heat. Tanuja et al. [9] explored the heat transference in three different fins with varying thermal conductivity. The results indicate that compared to the cylindrical shape, the concave parabolic profile improves heat transfer more efficiently. Optimizing triangular fins for enhanced heat transmission in forced convection was investigated by Shadlaghani et al. [10]. The findings indicate that triangular fins with a higher height-to-thickness ratio improved thermal performance by dissipating more heat. Khudhur et al. [11] utilized the experimental techniques to study straight parallel-fin with heat sinks that have been altered by incorporating or eliminating semicircular sections.

Among all the fin geometries, the convex parabolic fin is chosen for the current study due to its proven ability to enhance heat transfer by optimizing surface area and improving thermal performance in various conditions. Babaelahi and Eshraghi [12] work focuses on designing medical heat sinks with convex parabolic convective fin to maximize thermal performance. Convex parabolic fins have a significant impact on system efficiency and heat transfer rates under a variety of circumstances. Pirompugd and Wongwises [13] investigated the performance of convex parabolic fins under the partially wet conditions. In numerous real-world applications, including nuclear systems, biomedical implants, and microelectronic devices, heat is produced internally as a result of chemical reactions, electrical resistance, or volumetric energy sources. To preserve thermal control and system stability, heat conduction through fins is combined with the internal heat creation. To ensure dependable, secure operation and to precisely describe the thermal behavior of such systems, this internal heat generation must be taken into consideration. Hence, number of research have shown that how internal heat generation affects traditional fin forms like exponential, triangular, and rectangular fins [14–20].

This additional heat source alters the fin thermal behavior, intern which affects the efficiency of the fin. With a focus on the impact of geometric configuration on thermal performance, Liu et al. [21] conducted a theoretical and numerical study on the fin efficiency and effectiveness of printed circuit heat exchangers with straight channels. Sowmya et al. [22] conducted the comparative analysis of the efficiency of the different fin profile. They found triangular fin exhibits a faster temperature drop, while the rectangular and convex fin demonstrates higher efficiency. In an experimental study on rectangular fins in wet surroundings, Lin et al. [23] found that condensation effects significantly reduced wet fin efficiency. In a more recent study, Babitha and Madhura [24] investigated straight porous fins with variable thermal conductivity, emphasizing the influence of material characteristics on thermal performance and overall fin efficiency.

As the need for effective thermal management grows, researchers are looking into new working fluids to go along with creative fin shapes. Nanofluids have become an appealing option among all the other methods, because of their improved convective heat transfer and increased thermal conductivity. Nanofluids improve heat dissipation by making high heat flux systems more thermally conductive. The efficiency of heat transmission is greatly enhanced when finned surfaces are cooled using these nanofluids. In 1995, Choi and Eastman [25] initially proposed the idea of nanofluids. Later, numerous studies have shown that the combination of mono nanofluids with different fin shapes improves performance [26, 27]. Debnath and Pradhan [28] highlighted that shell-and-coil heat exchangers improve convective heat transfer by using nanofluids. But mono nanofluids have limitations regarding heat transmission and long-term stability, which led to the development of hybrid nanofluids. These hybrid nanofluids are obtained by combining two or more distinct types of nanoparticles suspended in a base fluid. Hosseinzadeh et al. [29] explored the thermal behavior of a moving porous concave parabolic fin wetted with a hybrid nanofluid in the presence of a magnetic field. The results demonstrate that the higher dimensionless temperatures resulting from quicker fin movement at higher Peclet numbers. Raju et al. [30] investigated how ternary hybrid nanofluids and convex fin profiles affected heat transfer behavior. Outcome shows that ternary hybrid nanofluids increase thermal conductivity which results in effective heat transfer. The impact of hybrid nanomaterials on heat transport and heat transfer fluctuations in blood flow systems was investigated by Iqbal et al. [31]. Heat dissipation is greatly improved by carefully combining ternary nanofluids with convex parabolic fins. For example, this design in solar panels reduces hotspots and increases energy output by removing additional heat from the backplate.

Also, effectively removes heat from vital parts of electronic gadgets, preserving consistent temperatures and averting thermal damage or overheating. Hence, ternary nanofluids are used to maximize thermal performance in a variety of industries, such as electronics, automotive cooling systems, and heat exchangers [32–37].

In thermal systems, the Local Thermal Equilibrium model (LTE) is frequently employed, presuming that the fluid and solid phases are in thermal equilibrium throughout the system. Moitsheki [38] analyzed the heat transmission in convex profiles, while taking temperature-dependent heat transfer coefficients and thermal conductivity into account. Based on thermo-geometric factors, the results indicate that convex fins produce higher efficiency. Kurtbaş et al. [39] experimentally investigated how the pressure drops, and heat transfer are affected by convex fins inside a rectangular channel at different Reynolds numbers. They confirmed that, in comparison to a smooth channel, convex fins greatly improve heat transport by 1.4 to 2.8 times. Nevertheless, when there are substantial temperature variations between the phases or in systems with intricate phase interactions such as nanofluids, this assumption is insufficient. In these situations, heat transmission cannot be reliably predicted by the LTE model. To overcome these difficulties, the LTNE model considers separate temperature fields for the solid and fluid phases, providing a more accurate depiction of heat transport in intricate systems. More recently, the Local Thermal Non-Equilibrium (LTNE) model offers a more accurate depiction of heat transmission than LTE in rectangular fin systems was discussed by Manaswini et al. [40].

Many studies have concentrated on specific elements of heat transfer such as fluid composition, fin geometry, and thermal modeling. However, there is a clear lack of research that simultaneously takes into account convex parabolic fins, ternary nanofluids, and LTNE conditions under both linear and nonlinear heat generation scenarios. In order to investigate their synergistic impacts on heat transfer optimization, this work adopts a novel strategy by integrating these components. An interesting practical application of this research is the utilization of fins in solar thermal collectors to enhance heat absorption from solar radiation and efficiently transfer it to working fluids. In such collectors, convex parabolic fins provide greater surface exposure while ternary nanofluids Go-Ag-Cu greatly enhance thermal conductivity of the base fluid. The nanoparticles like, Ag in the ternary nanofluid offers great thermal diffusivity and outstanding heat spreading capabilities, while Cu contributes strong thermal conductivity with good stability, and further, Go offers a wide surface area and excellent thermal conductivity. Hence, compared to single or binary nanofluids, these nanoparticles work well to improve overall heat transmission. The LTNE model is necessary for precise analysis since the solid and fluid phases may react differently to temperature changes under strong solar flux. Hence, this work enables improved thermal behavior prediction and optimization of fin. Also, combined effects of parameters on fin efficiency have not been thoroughly investigated in any prior studies, especially in systems that generate heat internally. Thus, the current study fills this knowledge gap by being the first to examine the LTNE model for convex parabolic fins in conjunction with ternary nanofluids, with an emphasis on fin efficiency. The findings offer a novel technique to boost thermal performance, heat dissipation, and system efficiency under LTNE conditions.

2. Mathematical model

This work considers a porous convex parabolic fin in one dimension with a variable cross-sectional area A^*_c and conduction of heat along the fin length L as shown in Figure 1. The fin outer surface dissipates thermal energy from the base which is maintained at a constant temperature T_b to the surrounding environment T_∞. In addition to the above presumptions, the analysis is performed under the following assumptions.

• The fin thickness is considered to be minimal compared to its other dimensions, so it is assumed that the temperature profile changes solely along with its length.

• The fin surface is infused with Go, Ag and Cu nanoparticles which are distributed in a conventional base fluid ethylene glycol-water mixture to improve convective and radiative heat transmission.

• To account for the fluctuation in heat production within the fin, the model includes both linear and nonlinear temperature-dependent internal heat generation.

• The interaction between the fluid and the solid matrix inside the porous fin is governed by the Darcy equation.

• Differential temperature gradients in the solid and fluid phases within the fin are permitted by the LTNE assumption.

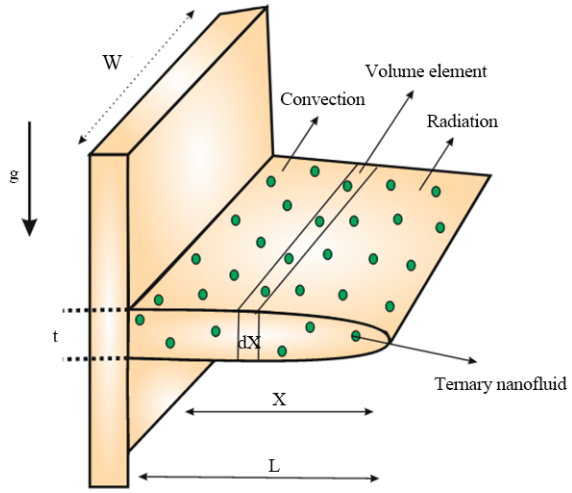


Figure 1. Convex parabolic fin

Based on the above-mentioned presumptions, the following equations (1)–(2) describe the energy balance for the fin (Tanuja et al. [33]):

Solid phase:

$$Q(X)-Q(X+\Delta X)+qA_c^*\Delta X \;= hP(1-\varphi)\,(T_s-T_\infty)\,\Delta X + h_{sf}A_{sf}\left(T_s-T_f\right) + P\sigma\varepsilon f_{f-a}\left(T^4{}_s-T^4{}_f\right)\Delta X + H_a i_{fg}A_{sf}\left(w_s-w_f\right). \tag{1}$$

Fluid phase:

$$Q(X)-Q(X+\Delta X)+qA_c^*\Delta X = M^* c_p\left(T_f-T_\infty\right)+h_{sf}A_{sf}\left(T_s-T_f\right). \tag{2}$$

The air mass flow rate via the porous fin is given by (Tanuja et al. [33]):

$$M^* = \rho_{tnf}\,(w.\Delta x)\,v_w. \tag{3}$$

Darcy equation is employed to represent the fluid-porous structure interaction and the subsequent fluid velocity driven by buoyancy in the porous media is represented by v_w which is defined below (Tanuja et al. [33]):

$$v_w = \frac{gK(\rho\beta)_{tnf}}{\mu_{tnf}}\left(T_f{}^*-T_\infty^*\right). \tag{4}$$

In the absence of radiation, the energy flux vector at the base is expressed as follows:

$$Q_{base} = Q_{con}+Q_{rad}. \tag{5}$$

Neglecting radiation and applying Fourier's law of conduction, we have:

$$Q_{cond} = -A_c^* k(T) \frac{dT}{dx}. \tag{6}$$

Since the heat transmission coefficients in real-world situations vary with temperature, internal heat generation is assumed to be fluctuate with temperature in both linear and non-linear forms. The expression for internal heat generation with a linear temperature dependence is given below (Girish et al. [41]),

$$q = q_a^* \left[1 + \varepsilon_g^* \left(T_s - T_f\right)\right] = q_a^* \left[1 + \varepsilon_g^* \left(T_f - T_s\right)\right]. \tag{7}$$

The expression for non-linear internal heat generation with a linear temperature dependence is given by (Girish et al. [41]),

$$q = q_a^* \left[1 + \varepsilon_g^* \left(T_s - T_f\right) + \varepsilon_{g1}^* \left(T_s - T_f\right)^2\right] = q_a^* \left[1 + \varepsilon_g^* \left(T_f - T_s\right) + \varepsilon_{g1}^* \left(T_f - T_s\right)^2\right]. \tag{8}$$

The nonlinear term ε_{g1}^* reflects sensitive heat effects in high-temperature or high-concentration locations, whereas the linear term ε_g^* compensates for base-level heating proportionate to temperature. These words physically represent the fin's temperature-dependent heat sources and localized energy dissipation. Based on tests and literature, typical ranges of $\varepsilon_g^* \left(0 \le \varepsilon_g^* \le 1\right)$ and $\varepsilon_{g1}^* \left(0 \le \varepsilon_g^* \le 1\right)$ are selected. The nonlinear radiation parameter ε_{g1}^* is typically smaller ($\approx$ 0.01-0.1) but becomes significant at high heat fluxes, whereas the linear radiation parameter ε_g^* typically ranges from 0.1-0.6 depending on surface emissivity and operating temperature in practical electronic cooling applications, such as processors and power modules.

By incorporating the necessary substitutions, the equations (1) and (2) are rewritten as follows:

Solid phase:

$$(1-\varphi)k_s \left[\frac{d}{dX} t(X) \frac{dT_s}{dX}\right] + \frac{16\sigma T_\infty^3}{3\beta_R} \left[\frac{d}{dX} t(X) \frac{dT_s}{dX}\right] + q = \frac{h_L p (1-\varphi)\left(T_s - T_\infty\right)\Delta X}{W * \Delta X} + \frac{h_{sf} A_{sf}}{W * \Delta X}\left(T_s - T_f\right)$$

$$+ \frac{4P\sigma\varepsilon f_{f-a}\left(T_s - T_\infty\right)\Delta X}{W * \Delta X} + \frac{H_a i_{fg} A_{sf}}{W * \Delta X}\left(w_s - w_f\right) = 0. \tag{9}$$

Fluid phase:

$$\varphi k_{tnf} \frac{d}{dx}\left(t(x)\frac{dT_{tnf}}{dx}\right) + q = \frac{A_{sf} h_{Sf}}{W\Delta X}\left(T_f - T_s\right) + \frac{(\rho C_p)_{tnf}\, gK(\rho\beta)_{tnf}}{W\mu_{tnf}\Delta X}\left(T_f - T_\infty\right)^2 \Delta X. \tag{10}$$

The convective boundary conditions for the current study are:

$$\begin{aligned} &\text{At } X=0 \qquad T_f(X)=T_s(X)=T_b \\ &\qquad\qquad -k_s\tfrac{dT_s}{dX}=h_s(T_s(L)-T_\infty) \\ &\text{At } X=L \\ &\qquad\qquad -k_f\tfrac{dT_f}{dX}=h_f(T_f(L)-T_\infty). \end{aligned} \tag{11}$$

Equations (9) and (10) are transformed into their respective nondimensional form by utilizing the nondimensional variables in equation (12) and thermophysical properties summarized in Tables 1 and 2.

$$\theta_s=\frac{T_s-T_\infty}{T_b-T_\infty},\theta_f=\frac{T_f-T_\infty}{T_b-T_\infty},X=\frac{x}{L}. \tag{12}$$

The equations for linear heat generation are expressed in the dimensionless form as follows:
Solid phase:

$$\left[X^{n-1}n[1+4R]\frac{d\theta_s}{dX}+X^n[1+4R]\frac{d^2\theta_s}{dX^2}\right]+Q\left[1+\varepsilon_G\left(\theta_s-\theta_f\right)\right]=\frac{2}{\tau}(\chi+Nr)\theta_s+m_2\left(\theta_s-\theta_f\right). \tag{13}$$

Fluid phase:

$$\left[X^{n-1}n\frac{d\theta_f}{dX}+X^n\frac{d^2\theta_f}{dX^2}\right]+Q\left[1+\varepsilon_G\left(\theta_f-\theta_s\right)\right]=\frac{1}{Z}\left(Bi\gamma\left(\theta_f-\theta_s\right)+Z_1\frac{Nc}{\tau^2}\theta_f^2\right). \tag{14}$$

The equations for non-linear heat generation are expressed in the dimensionless form as follows:
Solid phase:

$$\left[X^{n-1}n[1+4R]\frac{d\theta_s}{dX}+X^n[1+4R]\frac{d^2\theta_s}{dX^2}\right]+Q\left[1+\varepsilon_G\left(\theta_s-\theta_f\right)+\varepsilon_{G1}\left(\theta_s-\theta_f\right)^2\right]$$

$$=\frac{2}{\tau}(\chi+Nr)\theta_s+m_2\left(\theta_s-\theta_f\right)=0. \tag{15}$$

Fluid phase:

$$\left[X^{n-1}n\frac{d\theta_f}{dX}+X^n\frac{d^2\theta_f}{dX^2}\right]+Q\left[1+\varepsilon_G\left(\theta_f-\theta_s\right)+\varepsilon_{G1}\left(\theta_f-\theta_s\right)^2\right]=\frac{1}{Z}\left(Bi\gamma\left(\theta_f-\theta_s\right)+Z_1\frac{Nc}{\tau^2}\theta_f^2\right) \tag{16}$$

where,

$$Z=\left(\frac{k_1+2k_{tnf}-2\phi_1\left(k_{tnf}-k_1\right)}{k_1+2k_{tnf}+\phi_1\left(k_{hnf}-k_1\right)}\right)\left(\frac{k_2+2k_{nf}-2\phi_2\left(k_{nf}-k_2\right)}{k_2+2k_{nf}+\phi_2\left(k_{nf}-k_2\right)}\right)\left(\frac{k_3+2k_f-2\phi_3\left(k_f-k_3\right)}{k_3+2k_f+\phi_3\left(k_f-k_3\right)}\right)$$

$$Z_1 = \left(\left\{ (1-\phi_1) \left\{ (1-\phi_2) \left[(1-\phi_3) + \phi_3 \frac{(\rho\beta)_3}{(\rho\beta)_f} \right] + \phi_2 \frac{(\rho\beta)_2}{(\rho\beta)_f} \right\} + \phi_1 \frac{(\rho\beta)_1}{(\rho\beta)_f} \right\} \right)$$

$$\times \left(\{(1-\phi_1)\} \left\{ (1-\phi_2) \left[(1-\phi_3) + \phi_3 \frac{(\rho C_p)_3}{(\rho C_p)_f} \right] + \phi_2 \frac{(\rho C_p)_2}{(\rho C_p)_f} \right\} + \phi_1 \frac{(\rho C_p)_1}{(\rho C_p)_f} \right) \begin{pmatrix} (1-\phi_1)^{2.5} \\ \\ (1-\phi_2)^{2.5} (1-\phi_3)^{2.5} \end{pmatrix}.$$

The non dimensional boundary conditions for the current study are:

$$\theta_s(0) = \theta_f(0) = 1$$

$$\theta_f'[1] = -\frac{k_f}{k_{tnf}} Bi \left(\theta_f[1] \right), \theta_s'[1] = -\frac{k_f}{k_{tnf}} Bi \left(\theta_s[1] \right)$$

Table 1. Thermophysical properties (Girish et al. [41])

Properties	Go	Ag	Cu	Ethylene glycol-water 50-50%
ρ (kg/m^3)	1800	10500	4250	1063.8
k (W/m · K)	5000	429	8.9538	0.37
β (K^{-1})	0.00001	21	0.000076	0.00058
C_p (J/kg · K)	717	235	686.2	3630

Table 2. Thermophysical model of ternary nanofluid (Girish et al. [41], Mishra et al. [42])

Properties	Ternary Hybrid nanofluid
Density	$\rho_{tnf} = (1-\phi_1)\left\{(1-\phi_2)\left[(1-\phi_3)\rho_f + \phi_3\rho_3\right] + \phi_2\rho_2\right\} + \phi_1\rho_1$
Heat capacity	$(\rho C_p)_{hnf} = (1-\phi_2)\left[(1-\phi_1)(\rho C_p)_f + \phi_1 (\rho C_p)_1\right] + \phi_2 (\rho C_p)_2$
Viscosity	$\mu_{tnf} = \frac{\mu_f}{(1-\phi_1)^{2.5}(1-\phi_2)^{2.5}(1-\phi_3)^{2.5}}$,
Thermal conductivity	$\frac{k_{tnf}}{k_{hnf}} = \frac{k_1+2k_{tnf}-2\phi_1(k_{tnf}-k_1)}{k_1+2k_{tnf}+\phi_1(k_{hnf}-k_1)}$, where $\frac{k_{hnf}}{k_{nf}} = \frac{k_2+2k_{nf}-2\phi_2(k_{nf}-k_2)}{k_2+2k_{nf}+\phi_2(k_{nf}-k_2)}$, $\frac{k_{nf}}{k_f} = \frac{k_3+2k_f-2\phi_3(k_f-k_3)}{k_3+2k_f+\phi_3(k_f-k_3)}$
Electrical conductivity	$\frac{\sigma_{tnf}}{\sigma_{hnf}} = \frac{(1+2\phi_1)\sigma_1+(1-2\phi_1)\sigma_{hnf}}{(1-\phi_1)\sigma_1+(1+\phi_1)\sigma_{hnf}}$, where $\frac{\sigma_{hnf}}{\sigma_{nf}} = \frac{(1+2\phi_2)\sigma_2+(1-2\phi_2)\sigma_{nf}}{(1-\phi_2)\sigma_2+(1+\phi_2)\sigma_{nf}}$, $\frac{\sigma_{nf}}{\sigma_f} = \frac{(1+2\phi_3)\sigma_3+(1-2\phi_3)\sigma_f}{(1-\phi_3)\sigma_3+(1+\phi_3)\sigma_f}$,

3. Solution methodology

The differential equations are solved by various solution techniques [43–46]. In the present study, the nonlinear differential equations (13)–(16) have been converted from the general fin form to the convex parabolic fin by substituting $y = X^{1/2}$. Subsequently these equations are solved using the DTM, a semi-analytical method that was initially demonstrated by Zhou [47] and is derived from the Taylor series expansion. Additionally, the truncated DTM series

provides an approximate solution, its accuracy is deteriorated for larger values of the independent variable. Hence the Pade approximation is employed for better accuracy and convergence of the solution.

3.1 *The basic principles of DTM*

An infinitely and continuously differentiable function $Y(k)$ around any given point can be represented by a Taylor series expansion as follows:

$$Y(k)=\frac{1}{k!}\left[\frac{d^k y(x_0)}{dx^k}\right]_{y=0}, \tag{17}$$

and the corresponding inverse transformation of $Y(k)$ is represented by $y(k)$

$$y(k)=\sum_{k=0}^{\infty} Y(k)(x-x_0). \tag{18}$$

Equations (17) and (18) are combined to yield

$$Y(k)=\frac{1}{k!}\frac{d^k y(x_0)}{dx^k}(x-x_0)^k. \tag{19}$$

A finite series accurately depicts the result $Y(k)$, since the higher-order terms $Y(k)(x-x_0)$ are insignificant. As a result, the equation is expressed as below:

$$Y(k)=\sum_{k=0}^{n} Y(k)(x-x_0). \tag{20}$$

By altering the truncation order n and examining the ensuing temperature profiles, the convergence and consistency of the DTM solution for the entire model were carefully confirmed. It was verified that raising n above a particular threshold resulted in a slight variation in the profiles, suggesting that the solution has converged and is reliable.

The differential transform equation for linear heat generations (13) and (14) are obtained by utilizing equation (17) and (18) as follows:

Solid phase:

$$[1+4R]\sum_{r=0}^{k}\delta(r-1)(k-r+1)\Theta_s(k-r+1)-2[1+4R](k+1)\Theta_s(k+1)$$

$$+[1+4R](k+1)(k+2)\Theta_s(k+2)+Q\left[1+\varepsilon_G\left(\Theta_s(k)-\Theta_f(k)\right)\right]4\delta(r-1)$$

$$-\frac{2}{\tau}(\chi+Nr)\Theta_s(k)+4\delta(r-1)-m_2\left(\Theta_s(k)-\Theta_f(k)\right)4\delta(r-1)=0 \tag{21}$$

Fluid phase:

$$[1+4R]\sum_{r=0}^{k}\delta(r-1)(k-r+1)\Theta_f(k-r+1)-2[1+4R](k+1)\Theta_f(k+1)$$

$$+[1+4R](k+1)(k+2)\Theta_f(k+2)+Q\left[1+\varepsilon_G\left(\Theta_f(k)-\Theta_s(k)\right)\right]4\delta(r-1)$$

$$+\frac{1}{Z}\left(-Bi\gamma\left(\Theta_f(k)-\Theta_s(k)\right)-\frac{Z_1}{Z}\frac{Nc}{\tau^2}\sum_{r=0}^{k}\Theta_f(r)\Theta_s(k-r)\right)+4\delta(r-1)=0 \tag{22}$$

The differential transform equation for non-linear heat generation (15) and (16) are obtained by utilizing equation (17)–(18) as follows:

Solid phase:

$$[1+4R]\sum_{r=0}^{k}\delta(r-1)(k-r+1)\Theta_s(k-r+1)-2[1+4R](k+1)\Theta_s(k+1)+[1+4R](k+1)(k+2)\Theta_s(k+2)$$

$$+Q\left[1+\varepsilon_G\left(\Theta_s(k)-\Theta_f(k)\right)+\varepsilon_{G1}\sum_{r=0}^{k}\Theta_s(r)-\Theta_f(r)\left[\Theta_s(k-r)-\Theta_f(k-r)\right]\right]4\delta(r-1)$$

$$-\frac{2}{\tau}(\chi+Nr)\Theta_s(k)4\delta(r-1)-m_2\left(\Theta_s(k)-\Theta_f(k)\right)4\delta(r-1)=0 \tag{23}$$

Fluid phase:

$$[1+4R]\sum_{r=0}^{k}\delta(r-1)(k-r+1)\Theta_f(k-r+1)-2[1+4R](k+1)\Theta_f(k+1)+[1+4R](k+1)(k+2)\Theta_f(k+2)$$

$$+Q\left[1+\varepsilon_G\left(\Theta_f(k)-\Theta_s(k)\right)+\varepsilon_{G1}\sum_{r=0}^{k}\Theta_f(r)-\Theta_s(r)\left[\Theta_f(k-r)-\Theta_s(k-r)\right]\right]4\delta(r-1)$$

$$+\frac{1}{Z}\left(-Bi\gamma\left(\Theta_f(k)-\Theta_s(k)\right)-Z_1\frac{Nc}{\tau^2}\sum_{r=0}^{k}\Theta_f(r)\Theta_s(k-r)\right)4\delta(r-1)=0 \tag{24}$$

Reduced boundary conditions are:

$$\Theta_s[0]=\Theta_f[0]=1,\Theta_f[1]=a_1,\Theta_s[1]=a_2$$

$$\Theta_f[2]=-\frac{k_f}{k_{tnf}}Bi(a_1)$$

$$\Theta_s[2] = -\frac{k_f}{k_{tnf}} Bi\,(a_2) \tag{25}$$

Additionally, the values of $Y(k)$ (for $i = 1\ 2\ldots$) are found by substituting equation (20) into equations (21)–(24) and applying the recursive technique. The series solutions are then obtained by substituting these values into equation (17). Lastly, by assigning values to the physical parameters, equation (20) yields the final solutions with $n = 2$.

The physical interest of Derived quantities is:

$$Nu_s = \frac{q_s^* t}{k_{eq}\,(T_b - T_\infty)} = -\frac{(1-\varphi)kr}{\varphi + (1-\varphi)k}(1+4R)\Theta_s'(0), \tag{26}$$

$$Nu_f = \frac{q_f^* t}{k_{eq}\,(T_b - T_\infty)} = -\frac{(1-\varphi)\tau}{\varphi + (1-\varphi)k}\Theta_f'(0). \tag{27}$$

Equations (26) and (27) are added up to determine the rectangular permeable fin's overall Nusselt number for LTNE model:

$$Nu = Nu_s + Nu_f.$$

3.2 *Fin efficiency*

The ratio of the actual heat transfer from the fin to the amount of heat that would be transferred if the fin is at its base temperature is known as fin efficiency and is defined as;

$$\eta = \frac{\int_0^L \left(\frac{2}{\tau}(\chi + Nr)\theta_s - m_2\theta_s\right) dx}{\left(\frac{2}{\tau}(\chi + Nr) - m_2\right)}.$$

4. Graphical interpretations

A detailed semi-analytical investigation is conducted to examine the thermal properties of a convex parabolic fin in the presence of ternary nanofluids. Both linear and nonlinear temperature-dependent source functions are implemented to describe the fin internal heat generation. Further, separate fluid and solid temperature fields are considered by the LTNE assumption. The Rosseland approximation allows for the smooth integration of convective and radiative effects; Darcy's law demonstrates the fluid flow through the porous structure. The Differential Transform Method (DTM) is utilized to solve the resulting dimensionless equations semi-analytically. Although the DTM is adopted to address the LTNE model, the RKF45 and DTM approaches are employed for verifying the accuracy of the model against the rectangular fin scenario when $n = 0$ as shown in Table 3. Since there are no previous investigations on heat transfer analysis of convective parabolic fin under LTNE. Further, the temperature changes shown in the current theoretical analysis of fully wetted fins with a ternary nanofluid are similar to the major patterns reported in previous wetted-fin investigation by Lami et al. [46]. The overall thermal behavior is comparable with previously published data, even when nanofluid effects are taken into account. This agreement supports the reliability and validity of the theoretical model applied in this investigation. Table 4 indicates clearly that the ternary nanofluid exhibits improved thermal properties in comparison to the mono and hybrid nanofluids.

Table 3. Validation for current study when $n = 0, Q = \varepsilon_G = \varepsilon_{G1} = 0$

	$\theta_{fin-air}$					
X	0	0.1	0.3	0.6	0.9	1
Thimlapura Nagaraju et al. [48]	1	0.84031	0.60206	0.39388	0.31087	0.30167
Present study [RKF-45]	1	0.840306	0.602071	0.393637	0.310861	0.301651
Present study [DTM]	1	0.840321	0.602082	0.393636	0.310864	0.301615

Table 4. Comparison table for mono, hybrid and ternary nanofluids at $R = 2, Q = 0.5, Nr = 2, Nc = 0.1, \chi = 0.7, \tau = 1.5$

X	Θ					
	Mono-nanofluid		Hybrid-nanofluid		Ternary-hybrid nanofluid	
	Θ_s	Θ_f	Θ_s	Θ_f	Θ_s	Θ_f
0	1.	1.	1.	1.	1.	1.
0.1	0.980021	0.975026	0.980025	0.975031	0.980031	0.975039
0.2	0.960183	0.950233	0.960217	0.950278	0.960273	0.950351
0.3	0.940682	0.925878	0.940813	0.926053	0.941029	0.926345
0.4	0.921787	0.902322	0.922136	0.902802	0.922718	0.903617
0.5	0.903861	0.88007	0.904625	0.881147	0.905903	0.883
0.6	0.887391	0.8598	0.888851	0.861915	0.891294	0.865584
0.7	0.873012	0.8424	0.875532	0.846145	0.879718	0.852656
0.8	0.861539	0.828977	0.865508	0.835012	0.871987	0.845426
0.9	0.85397	0.820762	0.859613	0.829488	0.86854	0.844198
1	0.851074	0.818556	0.858135	0.829047	0.868387	0.846025

The impact of higher χ on Θ under both linear and nonlinear heat generation scenarios is illustrated in Figure 2a,b. Both the Θ_s and Θ_f temperatures decline as χ rises, the Θ_f drop being more noticeable under both case (a) and (b). In the case of nonlinear heat generation, the effect is more pronounced, particularly for the fluid phase. This demonstrates that the larger χ improves internal radiative transmission and lowers the fin internal heat resistance. Additionally, due to the extra ability to retain heat, the fin continuously keeps its temperature quite high. As χ increases, the equivalent fin efficiency falls, demonstrating its impact on thermal performance.

The temperature and heat distribution within the fin decrease as the wet porous parameter m_2 increases, as shown in Figure 3a,b. Higher wet porosity enhances moisture retention within the porous matrix, which increases thermal resistance and weakens heat coupling between the solid and fluid phases. As a result, the effective transport of thermal energy is suppressed, leading to a reduction in the temperature field throughout the fin. The results emphasize how crucial it is to balance heat retention and transfer efficiency in real-world applications, like solar thermal collectors or electronic cooling systems, by maximizing the wet porosity level. With this knowledge, designers can adjust the fluid saturation and porous structure for optimal thermal performance in a range of heat generating scenarios.

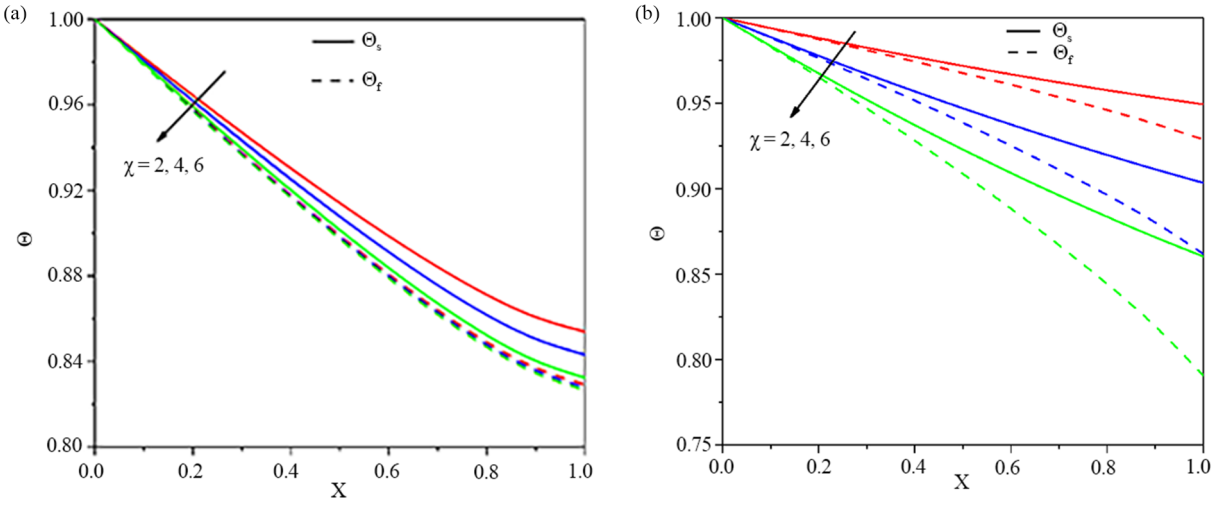


Figure 2. Impact of varying χ on Θ under both (a) Linear and (b) Non-linear heat generation

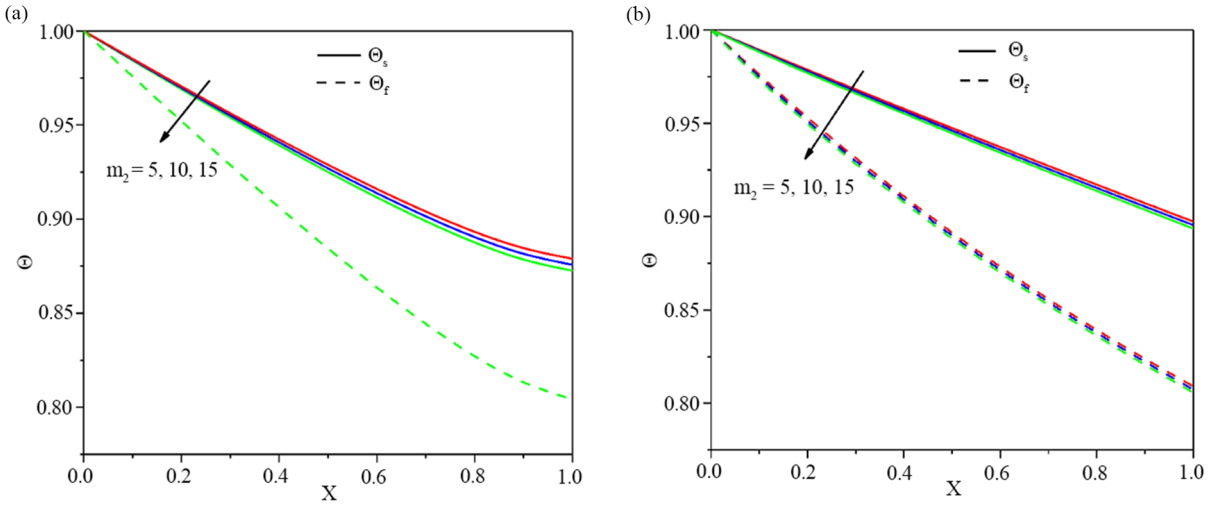


Figure 3. Impact of varying m_2 on Θ under both (a) Linear and (b) Non-linear heat generation

Natural convection becomes more intense as the *Nc* upsurges, causing heat to dissipate more quickly from Θ_s and Θ_f to ambient medium as shown in Figure 4a,b. The Θ_s cools more gradually in nonlinear heat generation scenarios as internal heating partially offsets convective losses, which results in a less noticeable temperature decline. On the other hand, the Θ_f loses heat more quickly due to its higher thermal conductivity and more effective convective heat transmission. In contrast, the cooling impact is more pronounced and uniformly spread across both phases in linear heat generation. Physically, this results in faster thermal equilibrium and more efficient heat dissipation, emphasizing the need of *Nc* in fin and system design for successful natural convection cooling.

Figure 5a,b illustrate how heat transfer through fin becomes more efficient as the *Nr* rises. Rapid cooling of both phases results from improved heat dissipation from the surface to the surrounding environment caused by advanced radiation. Also, internal heating intensifies the cooling effect in nonlinear heat generating scenarios. This causes a more noticeable drop in temperature than in linear heat generation, where the cooling effect is more uniform. Particularly for exposed or high-temperature systems, radiative heat loss is crucial in regulating the fin's thermal profile in addition to conduction and convection.

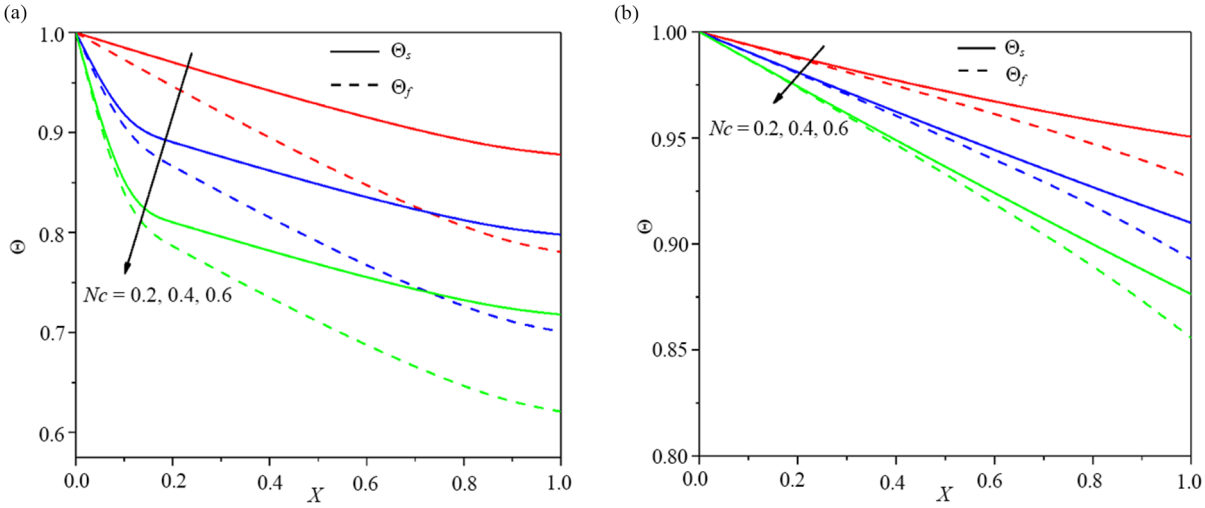


Figure 4. Impact of varying Nc on Θ under both (a) Linear and (b) Non-linear heat generation

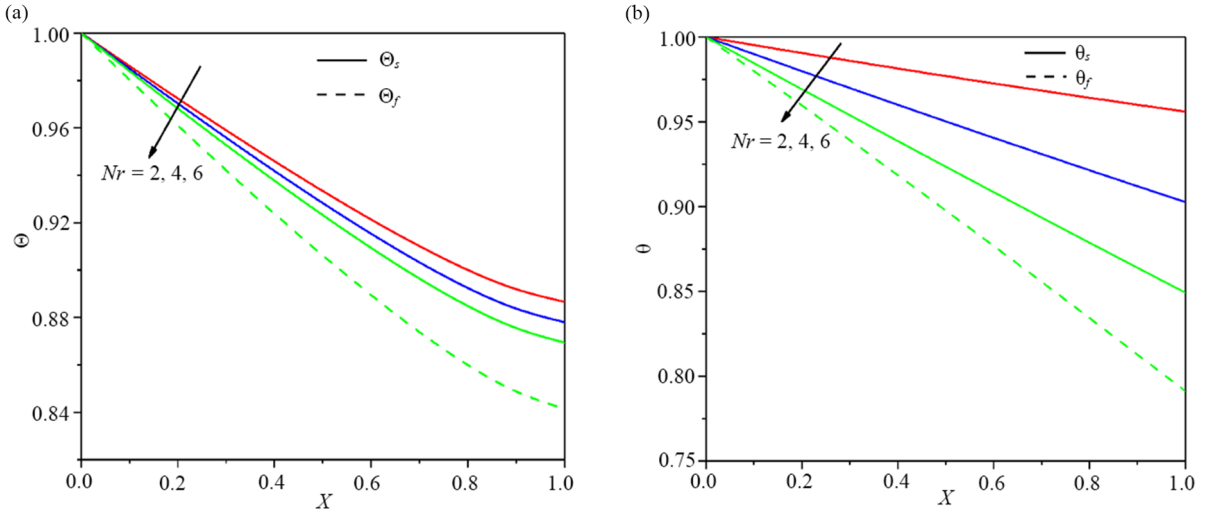


Figure 5. Impact of varying Nr on Θ under both (a) Linear and (b) Non-linear heat generation

The Θ_s and Θ_f grow in proportion to the ϕ as demonstrated in Figure 6a,b. Since the total concentration of nanoparticles is modest (≤3%). It is noted that the present model assumes a stable and uniform dispersion of nanoparticles and does not account for agglomeration or sedimentation effects. In practical applications, such phenomena may occur even at low nanoparticle concentrations and could influence the long-term thermal performance of the system. Hence, the agglomeration effects are negligible at such low densities. Although the Θ_s rise is more pronounced, suggesting a higher accumulation of thermal energy. The Θ_f is improved due to rise in nanoparticle concentration, which boosts heat transmission and fosters a stronger thermal connection between the solid and fluid phases. This stronger coupling promotes more effective heat distribution across the system and lowers convective losses. The increased internal heating caused by the enhanced thermal conductivity results in an even more noticeable temperature increase in the solid phase in nonlinear heat generation. Hence, without significantly altering the design, nanoparticles improve fin performance by strengthening the thermal connection between the solid and fluid phases.

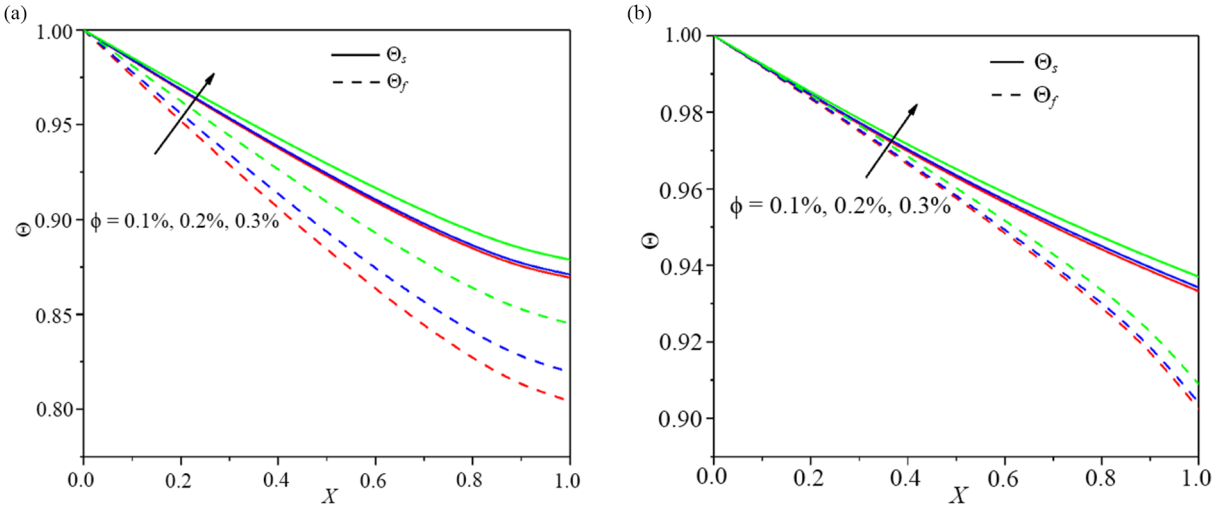


Figure 6. Impact of varying ϕ on $\theta(X)$ under both (a) Linear and (b) Non-linear heat generation

As Q increases, the temperatures Θ_s and Θ_f improve in both linear and nonlinear heat generation cases as displayed in the Figure 7a,b. The temperature rises smoothly in both solid and fluid phases in the linear scenario as heat generation rises steadily with temperature. Whereas, temperature rises more quickly and significantly in the nonlinear scenario due to more generation of heat. Compared to the fluid phase, the solid phase continuously holds more heat and remains hotter. Hence, impact of Q highlights how internal energy sources affect fin performance, demonstrating that excessive internal heat lower efficiency if it is not balanced by radiation or convection.

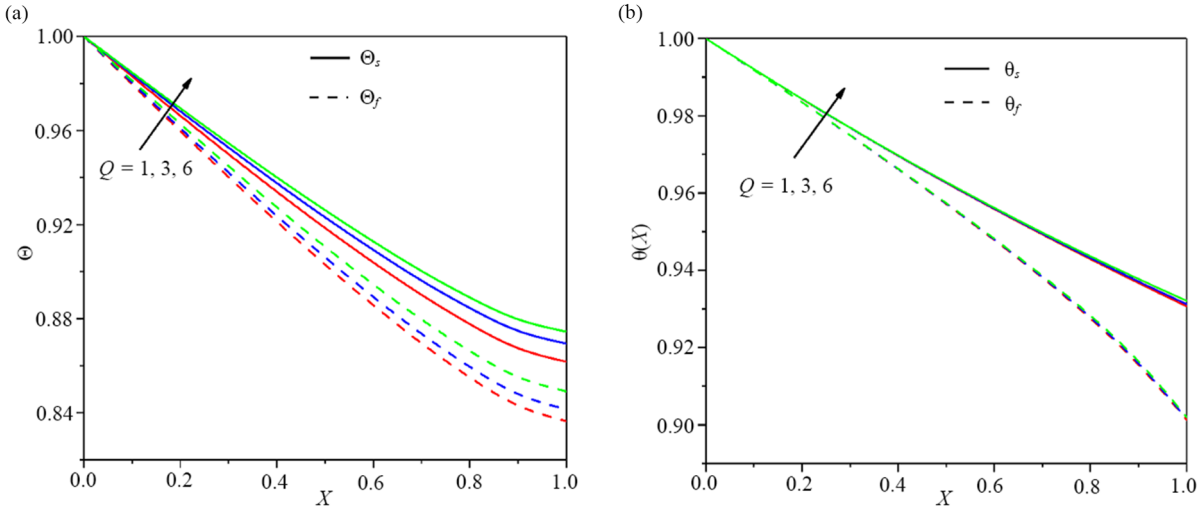


Figure 7. Impact of varying Q on Θ under both (a) Linear and (b) Non-linear heat generation

A greater radiation-conduction value boosts both the conductive heat transfer within the material and the heat exchange between the surface and the environment through radiation. Hence, Θ improves with an increase in radiation-conduction parameter as depicted in Figure 8a,b. The temperature rises as a result of conduction and radiation interacting to retain more heat inside the system and this rise is more in the case of nonlinear heat generation. Radiators and fins on spacecraft provide a real-world illustration of the radiation–conduction parameter. Fins must primarily radiate heat since there is no air for convective cooling in space, whereas conduction transfers heat from the spacecraft's body to the fin

surface. The efficiency of this heat transfer is determined by the radiation–conduction parameter; a high value prevents onboard systems from overheating by allowing the fin to radiate heat into space more effectively.

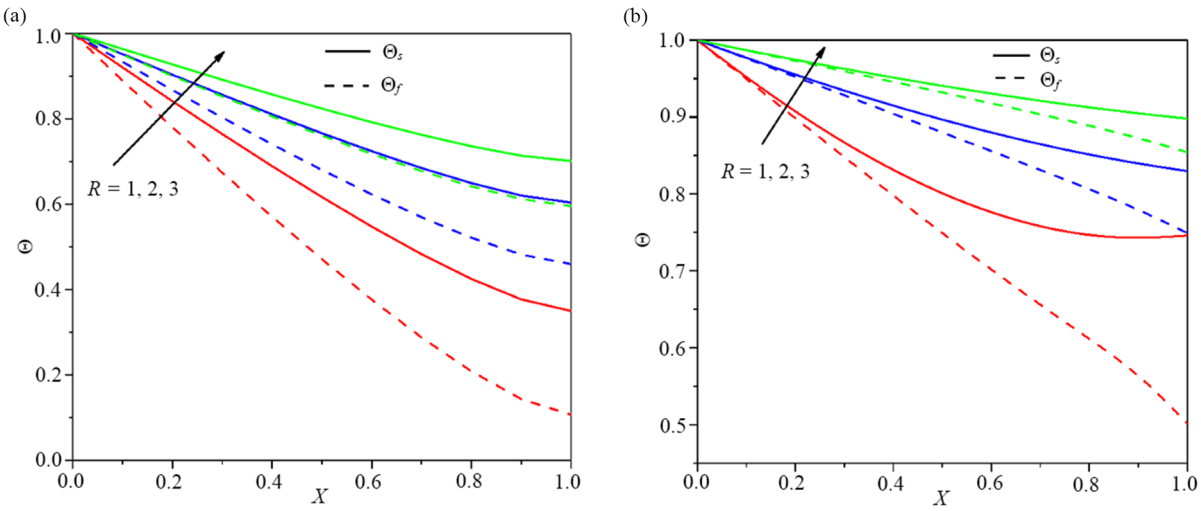


Figure 8. Impact of varying R on Θ under both (a) Linear and (b) Non-linear heat generation

The temperature of fluid and solid phase both grow due to rising τ as illustrated in Figure 9a,b. However, the solid region serves as the primary heat transporter which allows improved heat storage and lowers the rate of thermal loss. This effect is due to higher thermal capacity and direct heat conduction of the fin. In linear heat generation, both phases experience a moderate increase in temperature. When the thicker fin sustains more internal heating, the effect becomes stronger in nonlinear heat generation which results rise in Θ_s. In terms of structure, a thicker fin lowers thermal resistance and maintains higher temperatures along its length by allowing more heat to transfer from the base toward the tip.

The Figures 10–13 demonstrate crucial aspects of the fin called fin efficiency. Efficiency declines as τ rises owing to greater radiation losses from the larger surface area. Despite having more conductive area, this results in less efficient heat transfer overall. Convective heat transfer improves with growing χ which promotes heat dissipation from the fin to the surrounding fluid. As a result, the system is more efficient and has less heat resistance. On the other hand, heat loss to the environment becomes more prevalent as Nr rises. This lowers the efficiency of the system by transferring less heat to the solid phase. In a moist or porous fin, the internal resistance to heat transfer is represented by the wet porous parameter m_2. Due to greater thermal resistance, heat transfer efficiency falls as m_2 rises. The applications in the actual world illustrate this phenomenon of efficiency. For example, if a car radiator fin is extremely thin, heat will not transfer well and the tip will stay colder than the base, which would reduce efficiency. On the other hand, a fin that is optimally thick and has improved convection or radiation keeps its surface temperature higher along its length, which transfers more heat and increases efficiency.

Fin efficiency for rectangular, convex parabolic, and triangular fin profiles varies with the dimensionless length X as shown in Figure 14. The non-uniform distribution of cross-sectional area over the length causes the fin efficiency to vary considerably with the fin profile. Due to the decrease in the area toward the tip reduces heat loss and improves efficient heat transmission. Hence, rectangular fin has the lowest efficiency among the three profiles, while the triangular fin has the best efficiency, followed by the convex parabolic fin.

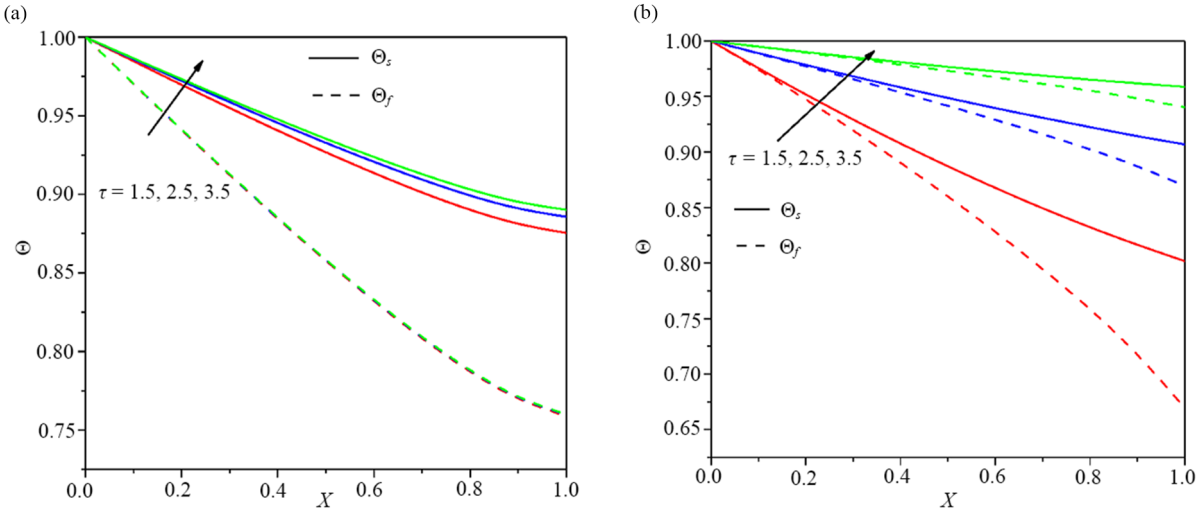


Figure 9. Impact of varying τ on Θ under both (a) Linear and (b) Non-linear heat generation

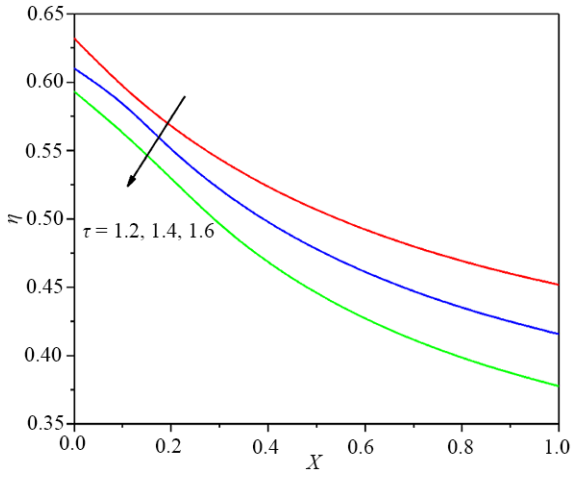


Figure 10. Impact of τ on η

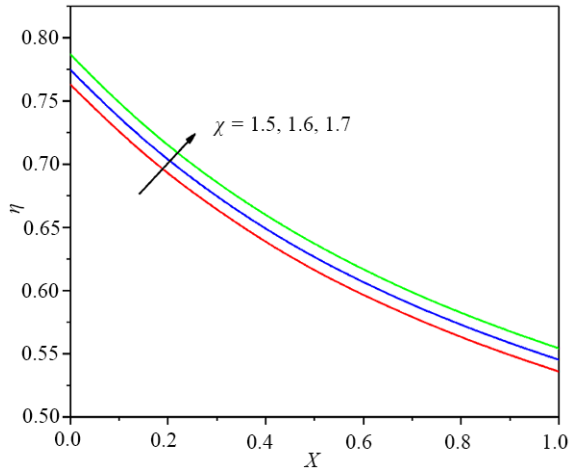


Figure 11. Impact of χ on η

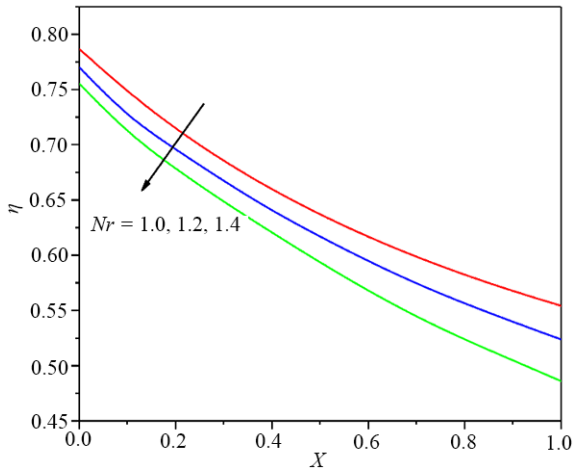


Figure 12. Impact of Nr on η

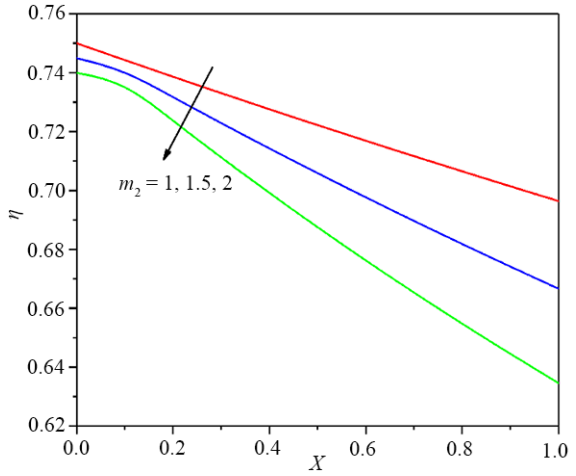


Figure 13. Impact of m_2 on η

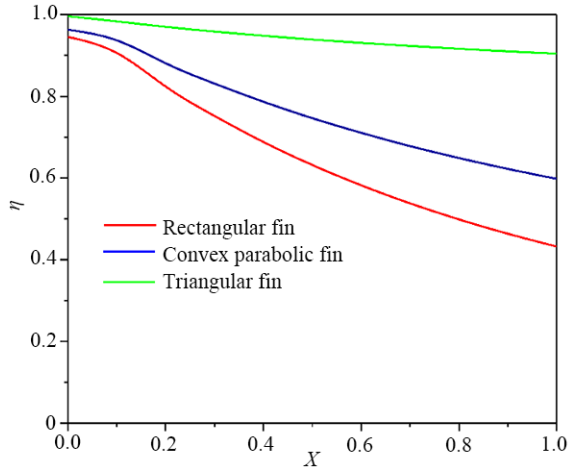


Figure 14. Impact of η on different fin profile

5. Conclusion

The thermal conductivity of a convex parabolic fin wetted in a ternary nanofluid inside a porous structure is investigated in this work. Further, both linear and nonlinear heat source components are incorporated in the model to more accurately reflect the complex nature of internal heat generation. The LTNE is considered to improve the accuracy of heat transfer analysis by incorporating temperature variations between the solid and fluid phase. The problem was solved semi-analytically by utilizing the Differential Transformation Approach. Below are the major findings of the study.

• The LTNE model clearly depicts the solid's superior heat storage capability, as indicated by the higher temperature sustained in the solid phase compared to the fluid phase.

• Temperature drops as the fin loses heat more quickly due to increased external convection and nonlinear radiation speeds up this cooling process even more.

• Heat transmission from the fin to the surroundings is reduced by higher wet porosity, which serves as a thermal barrier.

• A moderate nanoparticle concentration is $\leq 3\%$ which enhances thermal performance, whereas higher values induce agglomeration and reduce efficiency.

• Moderate fin thickness improves heat dissipation, while excessive thickness increases thermal resistance.

• In order to achieve an effective cooling, the parameters $m_2 \leq 0.1$, $\chi \leq 0.1$ and $Nr \leq 1$ is essential.

• Nanoparticles enhance the fin's ability to store heat, while internal heat generation supplies additional energy, increasing the overall temperature within the fin.

• The wet porosity and ambient radiation have an adverse effect on fin efficiency. Hence, keeping them, minimum is crucial to improving the fin's thermal efficiency.

• Fin temperatures are higher in nonlinear internal heat generation than in the linear case due to the uniform supply of energy.

• To improve and control fin thermal performance, future research focuses on time-dependent heat generation, smart or phase-change fins, magnetic or electric field effects, and multi-hybrid nanofluids.

• The one-dimensional model and constant base temperature assumption serve as limitations, but open opportunities for future studies to explore multi-dimensional geometries with realistic variable thermal boundaries for improved practical relevance.

Acknowledgments

The authors would like to thank Prince Sultan University, Saudi Arabia, for the technical support through the TAS research lab.

Author contributions

Manaswini R: Conceptualization, Methodology, Formal Analysis, Writing-Original Draft. S Manjunatha: Software, Validation, Visualization, Writing-Review & Editing. Khalil Ur Rehman: Methodology, Formal Analysis, Writing-Original Draft. Tanuja T N: Software, Writing-Review & Editing. Wasfi Shatanawi: Supervision, Formal Analysis, Writing-Review & Editing.

Funding

This research received no external funding.

Data availability

The datasets generated during and/or analyzed during the current study are available from the corresponding author on reasonable request.

Conflict of interest

The authors declare no competing financial interest.

References

[1] Harper RR, Brown WB. Mathematical equations for heat conduction in the fins of air-cooled engines. No. NACA-TR-158; 1923.

[2] Norris RH, Spofford WA. High-performance fins for heat transfer. *Transactions of the American Society of Mechanical Engineers*. 1942; 64(5): 489-495. Available from: https://doi.org/10.1115/1.4019155.

[3] Kiwan S, Al-Nimr MA. Using porous fins for heat transfer enhancement. *Journal of Heat Transfer*. 2001; 123(4): 790-795. Available from: https://doi.org/10.1115/1.1371922.

[4] Saedodin S, Sadeghi S. Temperature distribution in long porous fins in natural convection condition. *Middle-East Journal of Scientific Research*. 2013; 13(6): 812-817.

[5] Hatami M, Ganji DD. Investigation of refrigeration efficiency for fully wet circular porous fins with variable sections by combined heat and mass transfer analysis. *International Journal of Refrigeration*, 2014; 40: 140-151. Available from: https://doi.org/10.1016/j.ijrefrig.2013.11.002.

[6] Gorla RSR, Bakier AY. Thermal analysis of natural convection and radiation in porous fins. *International Communications in Heat and Mass Transfer*. 2011; 38(5): 638-645. Available from: https://doi.org/10.1016/j.icheatmasstransfer.2010.12.024.

[7] Madhavadas V, Das D, Mohta KA, Prabu SS. Comparative analysis on heat transfer of various fin profile using solid works: a systematic review. In: *IOP Conference Series: Earth and Environmental Science*. IOP Publishing; 2021. Available from: https://doi.org/10.1088/1755-1315/850/1/012029.

[8] Ravikumar M, Raj YA. Investigation of fin profile on the performance of the shell and tube heat exchanger. *Materials Today: Proceedings*. 2021; 45: 7910-7916. Available from: https://doi.org/10.1016/j.matpr.2020.12.745.

[9] Tanuja TN, Rehman KU, Kumar GV, Shatanawi W, Varma SVK, Asghar Z. On thermal performance of spine fin in magnetized hybrid fluid rooted with Cu and MoS_4 nanoparticles. *AIP Advances*. 2024; 14(1). Available from: https://doi.org/10.1063/5.0176878.

[10] Shadlaghani A, Tavakoli MR, Farzaneh M, Salimpour MR. Optimization of triangular fins with/without longitudinal perforate for thermal performance enhancement. *Journal of Mechanical Science and Technology*. 2016; 30: 1903-1910. Available from: https://doi.org/10.1007/s12206-016-0349-5.

[11] Khudhur DS, Al-Zuhairy RC, Kassim MS. Thermal analysis of heat transfer with different fin geometry through straight plate-fin heat sinks. *International Journal of Thermal Sciences*. 2022; 174: 107443. Available from: https://doi.org/10.1016/j.ijthermalsci.2021.107443.

[12] Babaelahi M, Eshraghi H. Optimum analytical design of medical heat sink with convex parabolic fin including variable thermal conductivity and mass transfer. *Extreme Mechanics Letters*. 2017; 15: 83-90. Available from: https://doi.org/10.1016/j.eml.2017.06.005.

[13] Pirompugd W, Wongwises S. Partially wet fin efficiency for the longitudinal fins of rectangular, triangular, concave parabolic, and convex parabolic profiles. *Journal of the Franklin Institute*. 2013; 350(6): 1424-1442. Available from: https://doi.org/10.1016/j.jfranklin.2013.02.019.

[14] Aziz A, Bouaziz MN. A least squares method for a longitudinal fin with temperature dependent internal heat generation and thermal conductivity. *Energy Conversion and Management*. 2011; 52(8-9): 2876-2882. Available from: https://doi.org/10.1016/j.enconman.2011.04.003.

[15] Mosayebidorcheh S, Farzinpoor M, Ganji DD. Transient thermal analysis of longitudinal fins with internal heat generation considering temperature-dependent properties and different fin profiles. *Energy Conversion and Management*. 2014; 86: 365-370. Available from: https://doi.org/10.1016/j.enconman.2014.05.033.

[16] Sobamowo MG. Analysis of convective longitudinal fin with temperature-dependent thermal conductivity and internal heat generation. *Alexandria Engineering Journal*. 2017; 56(1): 1-11. Available from: https://doi.org/10.1016/j.aej.2016.04.022.

[17] Minkler WS, Rouleau WT. The effects of internal heat generation on heat transfer in thin fins. *Nuclear Science and Engineering*. 1960; 7(5): 400-406. Available from: https://doi.org/10.13182/NSE60-A25737.

[18] Ünal HC. The effect of the boundary condition at a fin tip on the performance of the fin with and without internal heat generation. *International Journal of Heat and Mass Transfer*. 1988; 31(7): 1483-1496. Available from: https://doi.org/10.1016/0017-9310(88)90257-8.

[19] Sobamowo MG. Thermal analysis of longitudinal fin with temperature-dependent properties and internal heat generation using Galerkin's method of weighted residual. *Applied Thermal Engineering*. 2016; 99: 1316-1330. Available from: https://doi.org/10.1016/j.applthermaleng.2015.11.076.

[20] Sobamowo G. Finite element thermal analysis of a moving porous fin with temperature-variant thermal conductivity and internal heat generation. *Reports in Mechanical Engineering*. 2020; 1(1): 110-127. Available from: https://doi.org/10.31181/rme200101110s.

[21] Liu S, Huang Y, Wang J. Theoretical and numerical investigation on the fin effectiveness and the fin efficiency of printed circuit heat exchanger with straight channels. *International Journal of Thermal Sciences*. 2018; 132: 558-566. Available from: https://doi.org/10.1016/j.ijthermalsci.2018.06.029.

[22] Sowmya G, Gireesha BJ, Berrehal H. An unsteady thermal investigation of a wetted longitudinal porous fin of different profiles. *Journal of Thermal Analysis and Calorimetry*. 2021; 143: 2463-2474. Available from: https://doi.org/10.1007/s10973-020-09963-7.

[23] Lin YT, Hsu KC, Chang YJ, Wang CC. Performance of rectangular fin in wet conditions: visualization and wet fin efficiency. *Journal of Heat Transfer*. 2001; 123(5): 827-836. Available from: https://doi.org/10.1115/1.1391275.

[24] Babitha, Madhurab KR. Analysis of thermal performance, efficiency, and effectiveness of a straight porous fin with variable thermal conductivity. *Journal of Engineering Physics and Thermophysics*. 2022; 95(2): 392-401. Available from: https://doi.org/10.1007/s10891-022-02493-z.

[25] Choi SU, Eastman JA. Enhancing thermal conductivity of fluids with nanoparticles. No. ANL/MSD/CP-84938; CONF-951135-29. Argonne National Lab.; 1995.

[26] Jalili B, Aghaee N, Jalili P, Ganji DD. Novel usage of the curved rectangular fin on the heat transfer of a double-pipe heat exchanger with a nanofluid. *Case Studies in Thermal Engineering*. 2022; 35: 102086. Available from: https://doi.org/10.1016/j.csite.2022.102086.

[27] Khan ZH, Khan WA, Elbaz AM, Qasim M, Alharbi SO, Sun L. Natural convection in triangular fin-shaped cavity with partially heated base using nanofluid. *ZAMM-Journal of Applied Mathematics and Mechanics*. 2021; 101(12): e202000306. Available from: https://doi.org/10.1002/zamm.202000306.

[28] Debnath P, Pradhan M. A recent state of art review on heat transfer enhanced characteristics and material selection of SCTHX. *Proceedings of the Institution of Mechanical Engineers, Part E: Journal of Process Mechanical Engineering*. 2023; 237(3): 1005-1013. Available from: https://doi.org/10.1177/09544089221124463.

[29] Hosseinzadeh S, Hosseinzadeh K, Hasibi A, Ganji DD. Thermal analysis of moving porous fin wetted by hybrid nanofluid with trapezoidal, concave parabolic and convex cross sections. *Case Studies in Thermal Engineering*. 2022; 30: 101757. Available from: https://doi.org/10.1016/j.csite.2022.101757.

[30] Raju CSK, Sajjan K, Yook SJ. Heat transfer characteristics of rectangular/triangular/convex-shaped fins filled with hybrid nanoparticles under dry and wet conditions. *Physics of Fluids*. 2023; 35(11). Available from: https://doi.org/10.1063/5.0176926.

[31] Iqbal Z, Ahmad I, Khan SU, Kolsi L, Becheikh N, Ghachem K. Thermal analysis of hybrid nanofluid flow in blood vessels with peristalsis: case study for Hall current and radiative heat transfer. *Case Studies in Thermal Engineering*. 2025; 69: 105970. Available from: https://doi.org/10.1016/j.csite.2025.105970.

[32] Manaswini R, Hanumagowda BN, Tanuja TN, Kavitha L, Abdulrahman A, Punith Gowda RJ, Varma SVK. Sensitive analysis of heat transfer enhancement in ternary Casson nanofluid flow between a conical surface and disk. *Modern Physics Letters B*. 2025; 39(7): 2450420. Available from: https://doi.org/10.1142/S0217984924504207.

[33] Tanuja TN, Manjunatha S, Migdadi HS, Saadeh R, Qazza A, Khan U, Hussain SM, Yilmaz Y, Galal AM. Leveraging artificial neural networks approach for thermal conductivity evaluation in porous rectangular wetted fins filled with ternary hybrid nanofluid. *Journal of Radiation Research and Applied Sciences*. 2024; 17(4): 101125. Available from: https://doi.org/10.1016/j.jrras.2024.101125.

[34] Manjunatha S, Puneeth V, Gireesha BJ, Chamkha A. Theoretical study of convective heat transfer in ternary nanofluid flowing past a stretching sheet. *Journal of Applied and Computational Mechanics*. 2022; 8(4): 1279-1286. Available from: https://doi.org/10.22055/jacm.2021.37698.3067.

[35] Manjunatha S, Kuttan BA, Jayanthi S, Chamkha A, Gireesha BJ. Heat transfer enhancement in the boundary layer flow of hybrid nanofluids due to variable viscosity and natural convection. *Heliyon*. 2019; 5(4). Available from: https://doi.org/10.1016/j.heliyon.2019.e01469.

[36] Manjunatha S, Puneeth V, Anandika R, Gireesha BJ. Analysis of multilayer convective flow of a hybrid nanofluid in porous medium sandwiched between the layers of nanofluid. *Heat Transfer*. 2021; 50(8): 8598-8616. Available from: https://doi.org/10.1002/htj.22292.

[37] Khan SU, Ali MM, Tlili I, Bashir MN, Bani-Fwaz MZ, Khan Y, Hamida MBB. Non-linear thermal radiations impacts on entropy and heat transfer mechanisms in tetra nanofluid: investigation for Sakiadis model. *Journal of Radiation Research and Applied Sciences*. 2025; 18(3): 101750. Available from: https://doi.org/10.1016/j.jrras.2025.101750.

[38] Moitsheki RJ. Steady one-dimensional heat flow in a longitudinal triangular and parabolic fin. *Communications in Nonlinear Science and Numerical Simulation*. 2011; 16(10): 3971-3980. Available from: https://doi.org/10.1016/j.cnsns.2011.01.010.

[39] Kurtbaş İ, Yatağanbaba A, Şener M, Karakaş A. Heat transfer enhancement methods: concave and convex shape fins. In Proceedings of the 2nd World Congress on Mechanical, Chemical, and Material Engineering; 22-23 August 2016, Budapest, Hungary. Available from: https://doi.org/10.11159/htff16.129.

[40] Manaswini R, Manjunatha S, Chamkha AJ, Tanuja TN. A comparative heat transfer analysis of rectangular fin through LTE and LTNE model. *The European Physical Journal Plus*. 2025; 140(8): 787. Available from: https://doi.org/10.1140/epjp/s13360-025-06711-4.

[41] Girish R, Salma A, Subray PA, Hanumagowda BN, Varma SVK, Nagaraja KV, Chohan JS, Khan U, Hassan AM, Gamaoun F. Effect of temperature-dependent internal heat generation over exponential and dovetail convective-radiative porous fin wetted in hybrid nanofluid. *Case Studies in Thermal Engineering*. 2023; 49: 103214. Available from: https://doi.org/10.1016/j.csite.2023.103214.

[42] Mishra A, Pathak G, Kumar A. Computational analysis of bioconvection of MoS2-SiO2-GO/H2O ternary hybrid nanofluid containing gyrotactic microorganisms over an exponentially stretching sheet with chemical reaction. *BioNanoScience*. 2024; 14(2): 748-769. Available from: https://doi.org/10.1007/s12668-023-01279-8.

[43] Shahzad H, Batool H, Alghafli MA, Mlaiki N. Entropy generation and MHD flow characteristics of unsteady Williamson fluid toward a stagnation point over a vertical Riga plate. *Partial Differential Equations in Applied Mathematics*. 2025; 16: 101321. Available from: https://doi.org/10.1016/j.padiff.2025.101321.

[44] Asghar Z, Ashfaq M, Nie Y, Gondal MA. Comparative analysis of exact and FDM solutions with error analysis for thermal transport of copper-blood nanofluid in arteries with stenosis and thrombosis. *Thermal Science and Engineering Progress*. 2025; 68: 104178. Available from: https://doi.org/10.1016/j.tsep.2025.104178.

[45] Noreen S, Khan SA, Farooq U, Fatima N, Ali B, Muhammad T, Imran M. Numerical analysis of TiO2-SiO2-CuO/water-based ternary-hybrid nanofluid with thermal conductivity over a stretching wedge. *ZAMM - Journal of Applied Mathematics and Mechanics*. 2025; 105(11): e70277. Available from: https://doi.org/10.1002/zamm.70277.

[46] Al Lami J, Shourideh AH, Ajram WB, Haggag S, Mansouri A. Determination of temperature distributions of fully wet rectangular, triangular, and parabolic straight fins. *American Journal of Heat and Mass Transfer*. 2016; 3(5): 333-351. Available from: https://doi.org/10.7726/ajhmt.2016.1019.

[47] Zhou JK. *Differential Transformation and Its Applications for Electrical Circuits*. Wuhan: Huazhong University Press; 1986.

[48] Thimlapura Nagaraju T, Linganna K, Varma SV, Channaiah S, Kumar RSV, Khan U, Muhammad T, Abdou MMM. Thermal analysis of natural convection in rectangular porous fin wetted with CNTs nanoparticles and thermal radiation. *ZAMM - Journal of Applied Mathematics and Mechanics*. 2024; 104(8): e202300969. Available from: https://doi.org/10.1002/zamm.202300969.